Perspective

Abrupt climate change in the computer: Is it real?

Thomas F. Stocker* and Olivier Marchal

Climate and Environmental Physics, Physics Institute, University of Bern, Sidlerstrasse 5, CH-3012 Bern, Switzerland

Models suggest that dramatic changes in the ocean circulation are responsible for abrupt climate changes during the last ice age and may possibly alter the relative climate stability of the last 10,000 years.

Among the archives recording past climate and environmental changes, ice cores, marine and lacustrine sediments in anoxic environments, and tree rings have seasonal to annual resolution. Changes in dust level (1), snow accumulation (2), summer temperature (3), and indicators of the productivity of marine life (4) suggest that some of the climate changes have evolved on time scales as short as a few years to decades. Such changes appear abrupt in comparison with the classical view of climate change. The understanding of the mechanisms responsible for abrupt change has long relied on qualitative reasoning. However, climate research now increasingly makes use of numerical models as a tool to interpret and integrate results. Projections of anticipated climate change also rely on such models. Abrupt climate change, as recorded in many paleoclimatic archives (5), provides a challenge to these models. Their task is to elucidate the processes that are involved in abrupt change. If validated by the past, these models may be able to quantify the likelihood of future surprises in the climate system.

Ocean Circulation and Abrupt Change. Ocean currents cause significant geographical differences in the supply of heat to the atmosphere (6). Regions around the North Atlantic Ocean have a mean annual surface air temperature that is 5–7°C warmer than those at the same latitude in the Pacific. This is due to the thermohaline circulation (THC) of the Atlantic Ocean which is moving warm, saline tropical waters northward; the Gulf Stream is part of this basin-scale circulation. These tropical waters then give off their heat to the atmosphere north of Iceland, become denser and sink to the abyss, and flow southward in the form of a deep western boundary current (7). The two major locations of deep water formation in the Atlantic are in the Greenland-Iceland-Norwegian (GIN) Sea and in the Labrador Sea, both of which contribute to the formation of North Atlantic Deep Water. The THC is driven by differences in the density of sea water and therefore is controlled by the air–sea fluxes of heat and freshwater. In the Pacific there is no such circulation, because the surface waters are too fresh: even if cooled to the freezing point, they would not acquire enough density to sink down and establish a large-scale THC. This is caused by a combination of several factors, including reduced evaporation in the Pacific, fresher surface waters flowing northward, and a different basin geometry (8).

The Atlantic THC is a self-sustaining phenomenon and thus prone to instability. If the northward flow of saline tropical waters decreases (e.g., by increased river runoff, ice melt, changes in precipitation, etc.), the density of high latitude waters is reduced so that these waters are no longer able to sink: the circulation stops. The result is a very cool and fresh northern North Atlantic. This process, first described by the late Henry Stommel (9), is now well understood and found by most climate models (10–12). The thermohaline circulation can thus exhibit more than one stable equilibrium, a feature that is typical of a non-linear physical system.

The concept of hysteresis illustrates the possible responses of the ocean–atmosphere system to perturbations in the surface freshwater balance. More freshwater in the sinking regions reduces the THC (13–15) (Fig. 1). The system is stable and reacts in a linear fashion as long as threshold values are not crossed (Fig. 1*a*). An abrupt change with an amplitude that no longer scales with the perturbation occurs if threshold values are crossed (Fig. 1*b*). If the initial state of the ocean–atmosphere system is a unique equilibrium, the system jumps back to the original state once the perturbation has ceased: the abrupt change is reversible. However, if other equilibria exist, the perturbation causes an irreversible change (Fig. 1*c*). Hysteresis is well known in climate models, but its structure is highly model-dependent (16). A burning question is, Where are we now on the hysteresis, and what is its structure?

Where Models Agree with the Climate Record. Abrupt change is triggered in almost all climate models by perturbing the surface freshwater balance of the North Atlantic. By discharging freshwater, the thermohaline circulation reduces or collapses completely, but the response depends on the location, amplitude and duration of the perturbation (11, 12, 14, 15, 17, 18). All three responses shown in Fig. 1 can be generated in such models, albeit at different threshold values. The Younger Dryas cold event (12,700–11,550 years before present) is the most recent and best documented of the family of abrupt climate changes of the past. Large amounts of freshwater entered the ocean before Younger Dryas (19), which may have triggered this cold event. Models indicate that a full stop (10) or a reduction of the water flux associated with the THC to ≈20% of the modern value (11) both produce a drop in sea surface temperature in the North Atlantic of ≈8°C and a substantial cooling over Greenland of 4–10°C. Although the resolution of these coupled ocean–atmosphere models is still coarse, there is quantitative agreement with recent paleoclimatic estimates of temperature changes during that event (20).

Climate models provide much additional information if they also predict changes in the global carbon cycle. Recently, results from a climate–carbon cycle model have been directly compared with paleoclimatic data of the Younger Dryas (21). In response to a meltwater pulse (Fig. 2*a*), the model simulates a collapse of the THC in the Atlantic and a cooling whose timing agrees well with the Greenland ice core record (Fig. 2*b*). The amplitude of the cooling is too small by a factor of 4 because of the zonal averaging of the model. Slight warming during the northern cold event is simulated in the far south, evidencing the "bipolar seesaw" (22, 23) between northern and southern hemispheres (Fig. 2*c*). The atmospheric CO_2 concentration increases during the abrupt event, but the amplitudes do not exceed 30 parts per million by volume (Fig. 2*d*); this corresponds well with the CO_2 changes measured on ice cores (21, 24).

*To whom reprint requests should be addressed. E-mail: stocker@climate.unibe.ch.

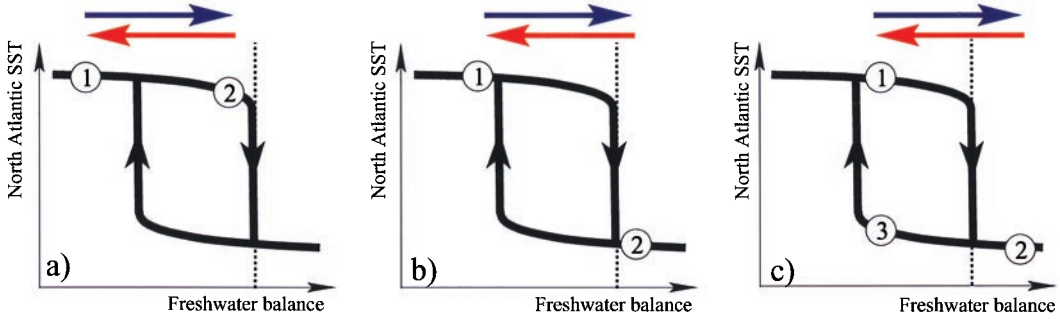

Fig. 1. The ocean–atmosphere system is a nonlinear physical system that can exhibit hysteresis behavior (13). The upper branch of the hysteresis is characterized by warm North Atlantic sea surface temperatures (SST), the lower branch by cold sea surface temperatures. A given perturbation (indicated by the blue and red arrows) in the freshwater balance of the North Atlantic (precipitation + runoff − evaporation) causes transitions from an initial state *1* to states *2* and/or *3*. Three structurally different responses are possible depending on whether threshold values (dashed line) are crossed: (*a*) Linear, reversible response. (*b*) Nonlinear, reversible response. (*c*) Nonlinear, irreversible response.

The stable isotopes of dissolved inorganic carbon in the ocean ($\delta^{13}C$) are further important variables in climate models that can be directly compared with the paleoclimatic record. In the deep North Atlantic, the climate–carbon cycle model simulates a decrease in $\delta^{13}C$ when the THC is reduced because surface waters rich in ^{13}C no longer sink to depth. This is in agreement with marine records that have sufficient resolution to identify this event (25). By contrast, $\delta^{13}C$ changes in the Southern Ocean are minor, again in agreement with the few available records (26).

It should be noted that the simulated changes to a given freshwater flux perturbation are strongly model-dependent, and mixing parameters like vertical diffusivities in the ocean models appear to be most influential (16).

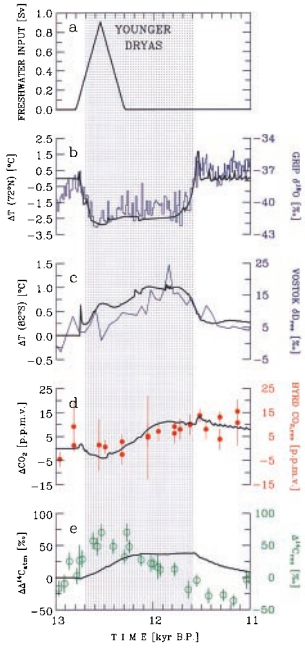

Fig. 2. Simulation and comparison with paleoclimatic data of the Younger Dryas cold event (shaded) using the climate–carbon cycle model of Marchal *et al.* (21). (a) Freshwater perturbation applied in the North Atlantic. (b) Reduction of surface air temperature at 72°N. Note that the duration of the event and the time scales of the cooling and warming agree well with the record from the Greenland ice core (blue), but this is strongly dependent on the little constrained freshwater input and therefore tunable. (c) Warming in the south consistent with isotope data from the Vostok ice core in Antarctica (blue). (d) Change in atmospheric CO_2 consistent with residual CO_2 values as measured on Byrd (red). p.p.m.v., parts per million by volume. (e) Change in atmospheric radiocarbon activity ($\Delta^{14}C$) showing disagreement with residual $\Delta^{14}C$ values from data of the Cariaco Basin (green). Details of the simulation and references to the data are given in ref. 21.

Where Models Disagree with the Climate Record. Models still have substantial difficulties in simulating important aspects of abrupt change when confronted with the hard evidence from the paleoclimatic archives. All current models respond instantaneously to a large perturbation in the freshwater balance, such as that used in Fig. 2. Yet, the sea level records tell us that the first meltwater peak during the deglaciation occurred ≈1,000 years before the onset of the Younger Dryas cold event (19). Little information is available about the locale of the freshwater discharge, and it may well be that the first meltwater pulse occurred around Antarctica, far away from the most vulnerable places with respect to the Atlantic THC (27). Some ice sheet melting must have occurred in the North Atlantic region, too, because ice rafted debris layers can be found right at the onset of Younger Dryas in high-resolution sediment cores from this basin (28). More detailed information about the timing and location of meltwater events is required for a comprehensive evaluation of model simulations of the Younger Dryas event.

A further disagreement with the paleoclimatic record is illustrated in Fig. 2*e*. Radiocarbon (^{14}C, half life 5,730 years, produced in the stratosphere from cosmic rays and oxidized to $^{14}CO_2$) is commonly used in geochronology. In addition, changes in the atmospheric ^{14}C activity, as recorded in tree rings or annually laminated marine sediments (4), can be used to estimate how efficiently the ocean transports ^{14}C from the surface to the abyss. Because the THC contributes to this transport, a collapsed THC would result in an accumulation of ^{14}C in the atmosphere. The paleoclimatic data show the expected increase of ^{14}C at the beginning of the Younger Dryas, but ^{14}C decreases already a few centuries later, long before the end of the event. This early decrease could be attributable to a significantly reduced production of radiocarbon in the stratosphere or a substantial increase in deep water formation in the Southern Ocean or elsewhere. No climate model is able to simulate this ^{14}C decrease at present.

Third, a full sequence of abrupt climate change such as seen in the Greenland ice core record (29) has not yet been simulated with climate models. Here the problems are twofold: (*i*) the initialization of such a model is an unresolved problem; and (*ii*) models of continental ice sheets, which will supply freshwater pulses, are only now being incorporated into comprehensive climate models. This field of coupled climate modelling is basically uncharted.

"Idealized" Abrupt Events. The increasing spatial coverage of, and new advances in, synchonizing paleoclimatic records have provided a clearer picture about how abrupt changes evolve. Ice cores from Greenland exhibit a sequence of 24 millennial events, the so-called Dansgaard/Oeschger events (D/O events) during the last ice age (10,000–110,000 years before present) (29). They are abrupt warmings followed by gradual coolings with temperature changes in Greenland of ≈10–16°C (Table 1). Comparison with the marine record suggests that the longest of these D/O events are preceded by so-called Heinrich events (H events) defined as ice rafted debris layers in North Atlantic sediments (28). The synchronization of Greenland and Antarctic ice cores suggests that a H event and the subsequent long D/O event form a unified sequence with associated global climate signals (24, 30). We call this sequence a "Heinrich-Dansgaard/Oeschger tandem" (H-D/O tandem). There are at least three, and likely five,

Table 1. Characteristics of Dansgaard/Oeschger (D/O) events and Heinrich (H) events

		Dansgaard/Oeschger event		Heinrich event
Characteristics				
Original definition		Abrupt change of $\delta^{18}O$ ratio in Greenland ice cores during last glaciation		Unusually high percentage of lithic fragments in coarse size fraction (thick IRD layers) in North Atlantic sediments during last glacial
Time scale		A few hundred to 2,000 years		More than 1,000 years
Recurrence time		About 2,000 years		About 7,000 years
Structure		Tend to come in bundles of three to four with decreasing recurrence time and duration, first in the bundle is significantly longer		Single event, precedes long D/O event
Further indicators				
Polar ice cores		CH_4		CO_2 (Antarctica)
Marine sediments		Thin IRD layers (North Atlantic), index of anoxia (Santa Barbara Basin), gray scale (Cariaco Basin), alkenones (Alboran Sea), magnetic susceptibility, and faunal abundances (Faeroe Margin)		Relative increase in faunal species indicating cooler conditions (North Atlantic); warming indicated by faunal species (South Atlantic)
Terrestrial records		Loess record (China)		Pollen abundances (lake in Florida), dryness index derived from pollen profiles (Colombia)
Spatial extent		Strongest in North Atlantic region, signals in entire northern hemisphere, weak or absent in southern hemisphere		Strong in North Atlantic but signals global, antiphase in southern hemisphere
Further climatic changes				
Temperature in North Atlantic region	√	Rapid warming (within decades), gradual cooling (within centuries)	√	Cold
North Atlantic Deep Water formation	?	Reduced or sites shifted (e.g., GIN Sea stopped, Labrador Sea active) before D/O, rapid switch-on of deep water formation in GIN Sea at D/O onset	?	Completely stopped
Low-latitude hydrological cycle	√	Wetter conditions		
North Atlantic Deep Water Export to Southern Ocean	?	No significant change	?	Stopped
Southern Ocean heat balance	?	No significant change	?	Heating
Bipolar seesaw	?	Not active	?	Active
Antarctic temperature	√	None	√	Slow Warming

The climatic changes marked with a check (√) are supported by paleo-data. The changes marked with (?) are still under debate and must be verified or falsified by additional data (see text). IRD denotes ice rafted debris.

examples of H-D/O tandems during the last glacial period (31).

H-D/O tandems are distinctly different from D/O events (Fig. 3). Only the former are associated with climate signals detected in Antarctica, which suggests that these events are of global extent and that there must exist an interhemispheric teleconnection mechanism that operates only during the H-D/O tandem (30). Furthermore, changes in atmospheric CO_2 concentration occur only during H-D/O tandems but not during D/O events (24, 31). The CO_2 changes are clearly correlated with the temperature changes recorded in the Antarctic ice cores (31) suggesting an important role for the Southern Ocean in influencing atmospheric CO_2.

Based on this, we propose the following scenarios of idealized D/O events and H-D/O tandems (Fig. 3). Before a D/O event, Greenland temperatures are cold. This implies that the THC is reduced and that probably deep water formation in the GIN Sea is largely reduced or stopped but it may continue elsewhere (south of Iceland and the Labrador Sea). D/O events would then be attributable to an abrupt switch-on of the Atlantic THC by resuming deep water formation in the GIN Sea. The warming would enhance the melting of the surrounding ice sheets leading to a subsequent reduction of the THC and associated cooling. The relatively short recurrence time of D/O events and small ice rafted debris layer thicknesses suggest that the amount of meltwater was not large. The partial shutdown, however, would be sufficient to induce a substantial cooling in the North Atlantic region. Because deep water formation is still active at other locations the changes in the THC are too small to activate teleconnections with the southern hemisphere (11). These events would thus go largely unnoticed there.

Why do the H-D/O tandems have a significantly longer recurrence time? We speculate that after a number of D/O events the accumulated meltwater caused a sea level rise that was sufficient to destabilize a large number of marine ice shelves (32). Once these shelves have broken loose, they would free the ice streams

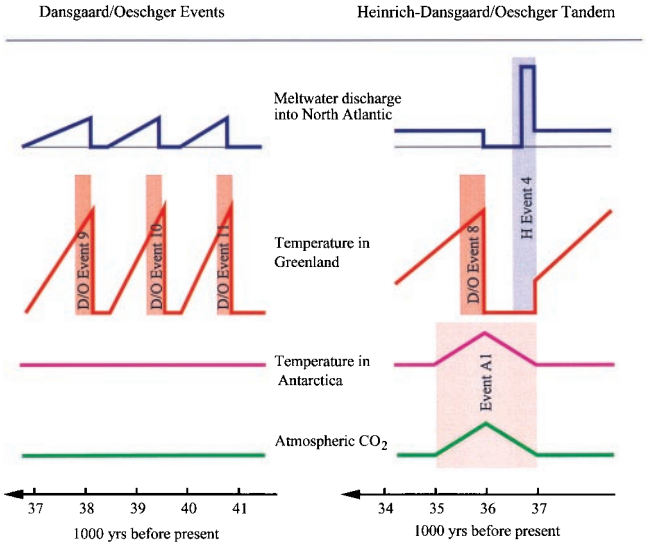

Fig. 3. Schematic view of a series of idealized Dansgaard/Oeschger events (*Left*) and an idealized Heinrich-Dansgaard/Oeschger tandem (*Right*) and as indicated in temperature changes in Greenland and Antarctic ice cores. Heinrich-Dansgaard/Oeschger tandems occurred at 14,500 years before present (H1, Bølling/Allerød warming), 36,000 years before present (H4 followed by D/O event 8), 45,000 years before present (H5 followed by D/O event 12), and probably at two earlier times (31).

behind them and a much larger meltwater discharge, an H event can be triggered. This would kill the THC completely and cause a massive cooling in the Atlantic region. Because the THC stops, heat is no longer exported from the Southern Ocean and a gradual warming occurs in the south. Therefore, an interhemispheric teleconnection via the Atlantic THC establishes a climatic change in antiphase with the north. This is the bipolar seesaw (22, 23) which is also simulated by climate models (10). According to this scenario, the warming in the south (event A1 in Fig. 3) is synchronous with the H event in the north. The change in the south is not abrupt because of the large heat capacity of the Southern Ocean. After a few centuries, the freshwater anomaly in the North Atlantic has been mixed away, sea surface density has increased, and the THC resumes. Models suggest that this switch-on is rapid. This would be registered as an abrupt warming in the north representing the D/O part of the H-D/O tandem. Heat is carried again northward by the Atlantic THC, and the temperature trend in the south reverses. Because of the large loss of ice mass at the H event, there would be several millennia of reduced melting activity. The D/O event of H-D/O tandem lasts, therefore, longer, and it would take some time until the next meltwater event occurs initiating the next bundle of D/O events. Abrupt events during the glacial would thus be reversible: Once the density anomalies caused by the meltwater event are removed, the THC resumes (Fig. 1*b*).

The proposed scenarios are based on the premise that the North Atlantic, through changes in the THC, triggers and determines the patterns of abrupt climate change with remote effects as far as Antarctica. On the other hand, the tropics are the Earth's heat engine and major supplier of water vapor, the most important greenhouse gas. It is where most of the energy from the sun is taken up and redistributed in the climate system. The role of the low latitudes for the dynamics of abrupt change has hardly been investigated (33). One low-latitude process with global teleconnections is El Niño/Southern Oscillation (ENSO). Temperature anomalies during a strong ENSO can easily reach 6°C as far distantas Central North America (33). ENSO also changes the surface freshwater balance of the Atlantic Ocean and could thus influence the THC (34). Whether ENSO was present during the glacial period or how ENSO was modified because of an altered seasonal cycle of solar radiation, lowered sea level and large continental ice sheets is unknown. Simulations with simplified models suggest that ENSO was active with unaltered spatial structure but modified frequency (35). Therefore, changes in the solar forcing would not affect the non-linear dynamics of the system but would influence the recurrence time of particular regimes (36). The latest generation of three-dimensional ocean–atmosphere models exhibit promising representation of ENSO (37) so that earlier hypotheses regarding the role of the tropics for abrupt climate change (38, 39) can be quantitatively investigated for the first time.

Conclusions. It should be stated clearly: Despite the many qualitative and sometimes quantitative agreements, there are serious gaps and shortcomings in our ability to simulate abrupt climate change. The shortcomings fall in two classes: (*i*) insufficiently known state of the climate system before and during these events, including forcing functions; and (*ii*) limited model resolution and representation of climate processes. They both need attention: first, by increasing the paleoclimatic database and aiming for high time resolution; second, by synchronizing the various records to better than 500 years; and, third, by developing an appropriate climate model hierarchy.

Can current models simulate abrupt climate change? Our answer is a partial yes. The necessary physics are in these models and allow for thresholds and switches of the THC. However, their location on the hysteresis now and in the past and the likely evolution of the THC in the future are unknown because we do not know whether there are additional stabilizing or destabilizing processes that we must take into account. Improvement is likely by the increase of grid resolution and better process representation in these models which is a natural development in step with the rise in computer power.

The lessons from the past are important for the future. Model simulations indicate the hydrological cycle gains in strength in a warmer climate (40, 41). Although the large continental ice sheets have long ceased to threaten the Atlantic THC, changes in evaporation and precipitation are likely to influence the THC and may be triggers of large ocean–atmosphere reorganisations in the future.

Comments by R. Alley are appreciated. Financial support of the Swiss National Science Foundation and the Swiss Federal Office of Education and Science is acknowledged.

1. Taylor, K. C., Lamorey, G. W., Doyle, G. A., Alley, R. B., Grootes, P. M., Mayewski, P. A., White, J. W. C. & Barlow, L. K. (1993) *Nature (London)* **361,** 432–436.
2. Alley, R., Meese D. A., Shuman, C. A., Gow, A. J., Taylor, K. C., Grootes, P. M., White, J. W. C., Ram, M., Waddingtong, E. D., Mayewski, P. A. *et al*. (1993) *Nature (London)* **362,** 527–529.
3. Björck, S., Kromer, B., Johnson, S, Bennike, O., Hammarlund, D., Lemdahl, G., Posnert, G., Rasmussen, T. L., Wohlfahrt, B., Hammer, C. U., *et al*. (1996) *Science* **274,** 1155–1160.
4. Hughen, K. A., Overpeck, J. T., Lehman, S. C., Kashgarian, M., Southon, J., Peterson, L. C., Alley, R. & Sigman, D. M. (1998) *Nature (London)* **391,** 65–68.
5. Broecker, W. S. (1997) *Science* **278,** 1582–1588.
6. Macdonald, A. M. (1998) *Prog. Oceanogr.* **41,** 281–382.
7. Dickson, R. R. & Brown, J. (1994) *J. Geophys. Res.* **99,** 12319–12341.
8. Weaver, A. J., Bitz, C. M., Fanning, A. F. & Holland, M. M. (1999) *Annu. Rev. Earth Planet. Sci.* **27,** 231–285.
9. Stommel, H. (1961) *Tellus* **13,** 224–241.
10. Schiller, A., Mikolajewicz, U. & Voss, R. (1997) *Clim. Dyn.* **13,** 325–347.
11. Manabe, S. & Stouffer, R. J. (1997) *Paleoceanography* **12,** 321–336.
12. Fanning, A. F. & Weaver, A. J. (1997) *Paleoceanography* **12,** 307–320.
13. Stocker, T. F. & Wright, D. G. (1991) *Nature (London)* **351,** 729–732.
14. Mikolajewicz, U. & Maier-Reimer, E. (1994) *J. Geophys. Res.* **99,** 22,633–22,644.
15. Rahmstorf, S. (1995) *Nature (London)* **378,** 145–149.
16. Manabe, S. & Stouffer, R. J. (1999) *Tellus Ser. A* **51,** 400–411.
17. Maier-Reimer, E. & Mikolajewicz, U. Technical Report 39, Max-Planck-Inst. für Meteorol., Hamburg, Germany, (1989) pp. 1–13.
18. Wright, D. G. & Stocker, T. F. (1996) in *Ice in the Climate System*, ed. Peltier, W. R. (Springer, Berlin), pp. 395–416.
19. Bard, E., Hamelin, B., Arnold, M., Montaggioni, L., Cabioch, G., Faure, G. & Rougerie, F. (1996) *Nature (London)* **382,** 241–244.
20. Severinghaus, J. P., Sowers, T., Brook, E. J., Alley, R. B. & Bender, M. L. (1998) *Nature (London)* **391,** 141–146.
21. Marchal, O., Stocker, T. F., Joos, F., Indermühle, A., Blunier, T. & Tschumi, J. (1999) *Clim. Dyn.* **15,** 341–354.
22. Broecker, W. S. (1998) *Paleoceanography* **13,** 119–121.
23. Stocker, T. F. (1998) *Science* **282,** 61–62.
24. Stauffer, B., Blunier, T., Dällenbach, A., Indermühle, A., Schwander, J., Stocker, T. F., Tschumi, J., Cappellaz, J., Raynaud, D., Hammer, C. U., *et al*. (1998) *Nature (London)* **392,** 59–62.
25. Boyle, E. (1995) *Philos. Trans. R. Soc. London B* **348,** 243–253.
26. Charles, C. D. & Fairbanks, R. G. (1992) *Nature (London)* **355,** 416–419.
27. Clark, P. U., Alley, R. B., Keigwin, L. D., Licciardi, J. M., Johnsen, S. J. & Wang, H. (1996) *Paleoceanography* **11,** 563–577.
28. Bond, G. C., Showers, W., Elliot, M., Evans, M., Lotti, R., Hajdas, I., Bonani, G. & Johnson, S. (1999) in *Mechanisms of Global Climate Change at Millennial Time Scales,* eds. Clark, P. U., Webb. R. S. & Keigwin, L. D. (Am. Geophys. Union, Washington, DC), pp. 35–58.
29. Dansgaard, W., Johnsen, S. J., Clausen, H. B., Dahl-Jensen, D., Gundestrup, N. S., Hammer, C. U., Hvidberg, C. S., Steffensen, J. P. Sveinbjornsdottin, A. E., Jouzel, J., *et al*. (1993) *Nature (London)* **364,** 218–220.
30. Blunier, T., Chappellaz, J., Schwander, J., Dällenbach, A., Stauffer, B., Stocker, T. F., Raynaud, D., Jouzel, J., Clausen, H. B., Hammer, C. U., *et al*. (1998) *Nature (London)* **394,** 739–743.
31. Indermühle, A., Monnin, E., Stauffer, B., Stocker, T. F. & Wahlen, M. (1999) *Geophys. Res. Lett,* in press.
32. McCabe, A. M. & Clark, P. U. (1998) *Nature (London)* **392,** 373–377.
33. Cane, M. A. (1998) *Science* **282,** 59–61.
34. Schmittner, A., Appenzeller, C. & Stocker, T. F. (1999) *Geophys. Res. Lett,* in press.
35. Clement, A., Seager, R. & Cane, M. (1999) *Paleoceanography* **14,** 441–455.
36. Corti, S., Molteni, F. & Palmer, T. N. (1999) *Nature (London)* **398,** 799–802.
37. Timmermann, A., Oberhuber, J., Bacher, A., Esch, M., Latif, M. & Roeckner, E. (1999) *Nature (London)* **398,** 694–697.
38. Heinrich, H. (1988) *Quat. Res.* **29,** 142–152.
39. McIntyre, A. & Molfino, B. (1996) *Science* **274,** 1867–1870.
40. Manabe, S. & Stouffer, R. J. (1993) *Nature (London)* **364,** 215–218.
41. Stocker, T. F. & Schmittner, A. (1997) *Nature (London)* **388,** 862–865.